DEVELOPMENT OF A WEAR MODEL FOR THE WHEEL PROFILE OPTIMIZATION ON RAILWAY VEHICLES RUNNING ON THE ITALIAN NET

M. Ignesti[1], A. Innocenti[1], L. Marini[1], E. Meli[1] and A. Rindi[1]

[1]Department of Energy Engineering, University of Florence
Via S. Marta n. 3, 50139 Firenze, Italy
e-mail: meli@mapp1.de.unifi.it

Keywords: multibody modeling of railway vehicles, wheel-rail contact, wheel-rail wear modeling, wheel-rail profile optimization

Abstract. *The reduction of wear due to wheel-rail interaction is a fundamental aspect in the railway field, mainly correlated to running stability and safety, maintenance interventions and costs. In this work the authors present two innovative wheel profiles, specifically designed with the aim of improving wear and stability behaviour of the standard ORE S1002 wheel profile matched with the UIC60 rail profile canted at $1/20$ rad, which represents the wheel-rail combination adopted in Italian railway line.*

The two wheel profiles, conventionally named CD1 and DR2, have been developed by the authors in collaboration with Trenitalia S.p.A. The CD1 wheel profile has been designed with the purpose of spreading the contact points in the flange zone on a larger area and having a constant equivalent conicity for small lateral displacements of the wheelset with respect to the centered position in the track. The DR2 wheel profile is instead designed in order to guarantee the same kinematic characteristics of the matching formed by ORE S1002 wheel profile and UIC60 rail profile with laying angle α_p equal to $1/40$ rad, widely common in European railways and characterized by good performances in both wear and kinematic behaviour.

The evolution of the wheel profiles due to wear has been evaluated through a wear model developed and validated by the authors in previous works with experimental data relative to the Aosta-Pre Saint Didier line.

In the present research the investigated trainset is the passenger vehicle ALSTOM ALn 501 "Minuetto", which is usually equipped with the standard ORE S1002 wheel profile and UIC60 rail profile canted at $1/20$ rad in Italian railways. The entire model has been simulated on a virtual track specifically developed to represent a statistical description of the whole Italian line. The data necessary to build this virtual track and the vehicle model were provided by Trenitalia S.p.A. and Rete Ferroviaria Italiana (RFI).

1 INTRODUCTION

Wear phenomena due to wheel-rail interaction represent a critical aspect in railway applications; in fact the consequent modifications in wheel and rail profiles may compromise the vehicle stability and dynamics. Profile changes lead also to higher maintenance cost, mainly concerned with the periodically re-profiling operations of wheels and the undesirable replacements of rails. The shape optimization of profiles for the reduction of wear at the wheel-rail interface represents so an important aspect in railway field and various approaches were developed to obtain a satisfactory combination of wheel and rail profiles. The optimum matching is usually pursued through the design of a new wheel profile which matches an existing rail profile, because the cost of rail interventions is notably higher compared with the cost of turning or replacement of the wheels.

This paper describes the design procedure and the behaviour in wear reduction of two innovative wheel profiles, developed by the authors in collaboration with Trenitalia and RFI, with the aim of reducing wheel-rail wear that occurs when coupling ORE S 1002 wheel profile and UIC60 rail profile with laying angle α_p equal to $1/20$ rad, as it occurs in Italian line. The two wheel profiles proposed in this paper are conventionally named CD1 wheel profile and DR2 wheel profile [19].

CD1 wheel profile has been designed starting from two different purposes. The first consists in distributing the contact points in the flange zone on a larger area in order to reduce wear phenomena. The second purpose is based on having a constant equivalent conicity value in a band around the initial contact point. The design procedure of DR2 wheel profile aims to keep with the new profile the kinematic characteristics of the matching formed by ORE S1002 wheel profile and UIC60 rail profile with laying angle α_p equal to $1/40$ rad, widely common in European railways and characterized by good performances in both wear and kinematic behaviour.

The evolution of wheel profiles has been evaluated through a model specifically developed for the wear assessment, which has previously been validated by the authors with experimental data relative to the Aosta-Pre Saint Didier line [4, 10, 15]. More specifically the developed model comprises two mutually interactive parts: the *vehicle model* (multibody model and 3D global contact model) and the *wear model* (local contact model, wear estimation and profiles updating).

The multibody model of the vehicle is implemented in the Simpack Rail environment and it takes into account all the significant degrees of freedom of the vehicle. The 3D global contact model, developed by the authors in previous works [4, 15], detects the wheel-rail contact points by means of an innovative algorithm based on suitable semi-analytical procedures and then, for each contact point, calculates the contact forces by means of Hertz's and Kalker's theory [9, 12, 14, 3, 11, 8, 16, 18]. Thanks to the numerical efficiency of the new contact model, it can interact directly online with the multibody model during the dynamic simulation of the vehicle, without look-up table (LUT) with saved pre-calculated values of contact parameters. Wear evolution is performed through a local contact model (in this case the Kalker's FASTSIM algorithm), an experimental relationship for the calculation of the worn material available in literature [6, 7, 17] (based on the work of the frictional forces) and a profile updating strategy. The wear model, starting from the outputs of the vehicle model (contact points, contact forces and global creepages), is able to calculate the total amount of removed material due to wear in dry conditions and its corresponding distributions along the wheel profile. Since the aim of the present research activity consists in the optimization of wheel profile, only wheel wear has been considered and the evolution of a single mean wheel profile for the whole vehicle is studied.

The dynamical simulations are performed on a virtual track, which has been designed to represent a statistical description of the whole Italian railway line [19]. This statistical railway line consists in a set of N_c radius classes; each class is characterized by a curvilinear track defined through specific radius R, superelevation h, velocity V and statistical weight p_k (with $1 \leq k \leq N_c$) values. A mean constant worn rail profile (in statistical sense) is then associated to each curvilinear track of the virtual track.

The trainset to be investigated in order to evaluate the capability in wear reduction of the two innovative profiles is the passenger vehicle ALSTOM ALn 501 "Minuetto", which is usually equipped with the standard ORE S1002 wheel profile and UIC60 rail profile canted at $1/20$ rad in Italian railway. This particular vehicle exhibits in fact severe wear and stability problems mainly caused by the adopted matching. The data necessary to build the multibody model of the vehicle and the virtual track model were respectively provided by Trenitalia S.p.A and RFI [19].

2 GENERAL ARCHITECTURE OF THE MODEL

The general architecture of the model consists in a discrete procedure articulated in two separate parts that work alternatively at each procedure step: the *vehicle model* and the *wear model*. The general layout of the entire model is illustrated in the diagram in Fig. 1.

The *vehicle model* is the part responsible for the dynamical simulations and it is based on the online mutual interaction of two sub-models, namely the multibody model of the vehicle to be investigated (in this work the ALSTOM ALn 501 "Minuetto") and the 3D global contact model. More specifically, at each integration step during time-domain dynamic simulation, the multibody model calculates the kinematic variables (position, orientation and their derivatives) of the considered vehicle at each wheelset. These variables are then passed to the 3D global contact model, the task of which consists in the calculation of the global contact parameters: contact points, contact areas, global creepages and contact forces. In particular, the contact points detection is based on an innovative algorithm developed by the authors in previous works [4, 15], while the contact forces (normal and tangential forces) calculation is performed according to Hertz's and Kalker's global theories [9, 12, 14]. Once the tangential contact problem has been solved, the values of the global forces are sent back to the multibody model and the dynamical simulation proceeds with the next time integration step. During this research project, according to the specifications required by Trenitalia, the capability on wear reduction of two innovative wheel profiles has been evaluated. Each of these profiles (CD1 and DR2 wheel profiles designed by the authors in collaboration with Trenitalia and RFI [19]) fits the considered vehicle in a specific simulation set.

The *wear model* is the part of the procedure concerning the computation of wheel profile evolution and it predicts the amount of worn material to be removed from the wheel surfaces. The wear model can be sub-divided into three parts: the local contact model, the evaluation of worn material and the profile updating. Firstly, the local contact model (based on Hertz's local theory and Kalker's simplified theory implemented in FASTSIM algorithm) estimates the local contact pressures and creepages and detects the creep zone of the contact area. Then, according to an experimental relationship between the worn material and the energy dissipated by friction forces at the contact interface available in literature [6, 7, 17], the quantity of removed material on wheel surface is computed on the creep area. This estimation is performed hypothesizing dry contact friction at the wheel-rail interface as Trenitalia and RFI requirements establish. Last step of the wear prediction procedure consists in updating the profiles: the worn profiles are derived from the original ones using an appropriate update strategy. The single mean profile
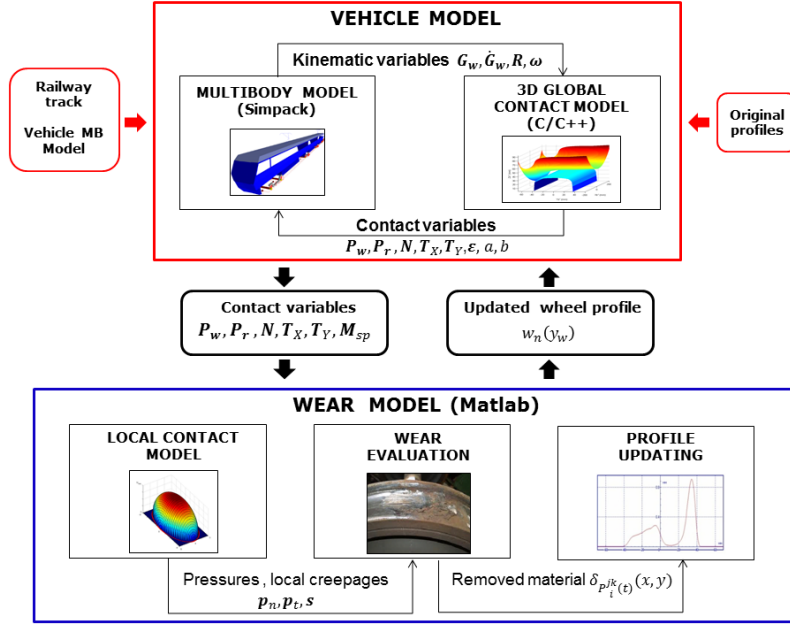
Figure 1: General architecture of the model.

(the same one for all the vehicle) is then fed back as input to the entire *vehicle model* and the whole model procedure proceeds with the next discrete step.

The adopted updating strategy is a key point since it may appreciably affects the results and its main task consists in choosing the appropriate discrete steps for the update of wheel profiles. Two different strategies are available in literature, differing each other for the choice of the discrete step which has to consider the influence of the run distance by the investigated vehicle km_{tot}. These strategies are the constant step update strategy, which is characterized by a constant value km_{step} of the discrete step and the adaptive step update strategy, wherein the profile is updated when a given threshold of the maximum value of cumulative wear depth is reached and the value km_{step} is consequently variable. During this research activity the adaptive step has been adopted for its capacity in representing the non-linear wear evolution (particularly in the first phase of the simulations, characterized by non-conformal wheel-rail contact). Furthermore, this strategy presents computational times comparable with those characterized by a constant step.

3 THE VEHICLE MODEL

The present section deals with the description of the *vehicle model*. First of all the multibody representation for the dynamical simulations of the studied vehicle is introduced. Then the algorithm that models the 3D global contact is explained. The trainset investigated during this research is ALSTOM ALn 501 "Minuetto", a passenger transport unit widespread in Italian Railways, equipped with the standard ORE S1002 wheel profile which matches the UIC60 rail profile canted at $1/20$ rad. This particular vehicle exhibits in fact severe wear and stability problems mainly caused by the adopted matching. Its mechanical structure and inertial, elastic and damping properties can be found in literature [19]. The Tab. 1 shows the main characteristics of the considered vehicle.

The multibody model of the vehicle has been implemented in the Simpack environment and it consists of thirty-one rigid bodies: three coaches, four bogies (two external motor bogies and
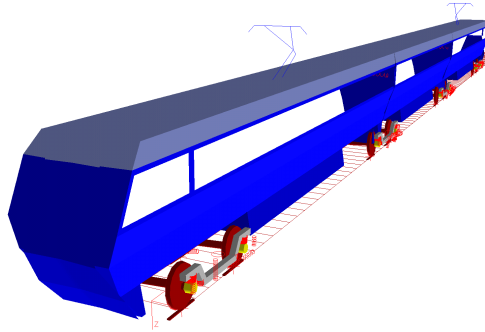
4

Figure 2: Global view of the multibody model.

two intermediate trailer bogies interposed between two successive coaches), eight wheelsets (two for each bogie) and sixteen axleboxes. The dual-stage suspensions have been modelled by

Table 1: Main characteristics of the Aln 501 Minuetto DMU.

Length	51.9 m
Width	2.95 m
Height	3.82 m
Bogie pivot distances	14.8-13.8-14.8 m
Bogie wheelbase	2.80 m
Unladen weight	100 t
Wheel arrangement	Bo-2-2-Bo
Wheel diameter	850 mm
Max speed	130 km/h

means of three-dimensional linear and non linear visco-elastic force elements. In the primary suspension stage the elastic elements are Flexicoil springs (constituted by two coaxial helical compression springs), while damping of the vertical relative displacement is provided by means of two non linear dampers. The secondary stage is formed by pneumatic suspensions and it comprises the following elements: two air springs, six non linear dampers (lateral, vertical and anti-yaw dampers), one non linear traction rod, the roll bar and two non linear lateral bumpstops.

In this research activity a specifically developed 3D global contact model has been used in order to improve reliability and accuracy of the contact points detection, compared to those given by the Simpack Rail contact model. More specifically, the adopted contact model is based on a two step procedure; at the first step the contact points number and positions are computed by means of an innovative algorithm designed and validated by the authors in previous works [4, 15]. During the second step, for each detected contact point, the global contact forces are evaluated using Hertz's and Kalker's global theories [9, 12, 14]. The contact point detection algorithm is a 3D algorithm that takes into account all the six relative degrees of freedom (DOF) characterizing the wheel-rail interaction; it also enables the analysis of generic railway tracks and wheel-rail profiles without introducing kinematic or geometrical problem simplification for the multiple contacts. The innovative algorithm does not impose any condition on the number of detected points and it is characterized by an high numerical efficiency that allows the on-line implementation in the commercial Multi-Body Simulation (MBS) software (Simpack-Rail, Adams-Rail) without look-up table (LUT) with saved pre-calculated values of contact parameters [5].

4 THE WEAR MODEL

The current section deals with the description of the three phases constituting the wear model: the local contact model, the computation of the amount of worn material (assuming dry contact conditions) and the wheel profile update.

The inputs of the wear model are the global contact parameters estimated by the vehicle model. Since a local wear computation is required, the global contact parameters need to be post-processed and this can be achieved with the simplified Kalker's theory implemented in the FASTSIM algorithm. This theory starts from the global creepages (ε), the normal and tangential global forces (N^r, T_x^r, T_y^r), the contact patch dimensions (a, b) and the material properties to compute the local distribution of normal p_n and tangential $\mathbf{p}_t$ stresses and local creepages $\mathbf{s}$ across the wheel/rail contact area. For a more detailed description of the FASTSIM algorithm one can refers to the literature [13].

The distribution of worn material on wheel profile due to wear (assuming dry contact conditions) is computed by means of a wear experimental function, based on a law that relates the energy dissipated in the wheel-rail contact patch with the amount of worn material [6, 7]. The adopted wear function uses local contact tangential $\mathbf{p}_t$ stresses, creepages $\mathbf{s}$ and the vehicle velocity V as the input to compute directly the specific volume of worn material $\delta_{P_{wi}^{jk}(t)}(x, y)$ (mm^3/mm mm^2) related to the i-th contact point $P_{wi}^{jk}(t)$ on the j-th wheel relative to the k-th dynamical simulation from the N_c simulations defined by the statistical analysis, for unit of distance travelled by the vehicle (expressed in m) and for unit of surface (expressed in mm). The x and y coordinates describes respectively the longitudinal and lateral position of a generic point within contact area. Local contact stresses and creepages are used to evaluate the *wear index* I_W (expressed in N/mm^2), which represents the frictional power developed by the tangential contact pressures: $I_W = \frac{\mathbf{p}_t \bullet \mathbf{s}}{V}$.

This index can be correlated with the *wear rate* K_W which represents the mass of removed material (expressed in µg/m mm^2) for unit of distance travelled by the vehicle and for unit of surface. The correlation is based on real data available in literature [6], which have been acquired from experimental wear tests carried out in the case of metal to metal contact with dry surfaces using a twin disc test arrangement.

The experimental relationship between K_W and I_W chosen for the development of the present wear model is described by the following equation:

$$K_W(I_W) = \begin{cases} 5.3 * I_W & I_W < 10.4 \\ 55.12 & 10.4 \leq I_W \leq 77.2 \\ 61.9 * I_W - 4778.68 & I_W > 77.2. \end{cases} \tag{1}$$

Once the wear rate $K_W(I_W)$ has been computed, the corresponding specific volume of worn material (for unit of distance travelled by the vehicle and for unit of surface) can be calculated as follows (expressed in mm^3/m mm^2):

$$\delta_{P_{wi}^{jk}(t)}(x, y) = K_W(I_W)\frac{1}{\rho} \tag{2}$$

where ρ is the material density (expressed in kg/m^3).

After obtaining the amount of worn material, wheel profile need to be updated and then it can be used as the input of the next dynamic simulation. The new profile, denoted by $w_n(y_w)$, is computed from the old one $w_o(y_w)$ and from all the calculated distributions $\delta_{P_{wi}^{jk}(t)}(x, y)$ of worn

material through an appropriate set of numerical procedures that defines the update strategy. The update strategy is also applied with the aim of reducing the numerical noise characterizing the distributions $\delta_{P_{wi}^{jk}(t)}(x, y)$ that can generate problems to the global contact model because of the presence of non physical alterations in new profiles. Another issue to be provided from the update procedure is the average of the worn material distributions. In fact, according to Trenitalia and RFI requirements, the output of the wear model must be a single profile for the entire vehicle model; hence the evaluated distribution $\delta_{P_{wi}^{jk}(t)}(x, y)$ needs to be mediate.

The whole numerical procedures which computes the new profiles can be summed up in the following steps:

1. *Longitudinal integration*:

$$\frac{1}{2\pi w(y_{wi}^{Cjk})} \int_{-a(y)}^{+a(y)} \delta_{P_{wi}^{jk}(t)}(x, y)dx = \delta_{P_{wi}^{jk}(t)}^{tot}(y) \tag{3}$$

the previous integration provides the mean value of wheel worn material in longitudinal direction expressed in mm^3/m mm^2. More specifically the operation sums in the longitudinal direction all the wheel wear contributions inside the contact path and distributes the resulting quantity along the wheel circumference of length $2\pi w(y_{wi}^{Cjk})$.

2. *Time integration*:

$$\int_{T_i}^{T_e} \delta_{P_{wi}^{jk}}^{tot}(y)V(t)dt \approx \int_{T_i}^{T_e} \delta_{P_{wi}^{jk}}^{tot}(s_w - s_{wi}^{cjk}(t))V(t)dt = \Delta_{P_{wi}^{jk}}(s_w) \tag{4}$$

where the natural abscissa s_w relative to the curve $w(y_w)$ has been introduced. The following relations locally hold (see Fig. 3):

$$y \approx s_w - s_{wi}^{cjk}(t) \qquad w(y_w) = w(y_w(s_w)) = \tilde{w}(s_w). \tag{5}$$

The natural abscissa of the contact point s_{wi}^{cjk} can be evaluated starting from its position P_{wi}^{jk}, in particular from y_{wi}^{Cjk}. Therefore the integration (4) sums all the wear contributions relative to the dynamic simulation and gives as output the depth of worn material due to the considered contact point $\Delta_{P_{wi}^{jk}}(s_w)$ in mm=mm^3/mm^2.
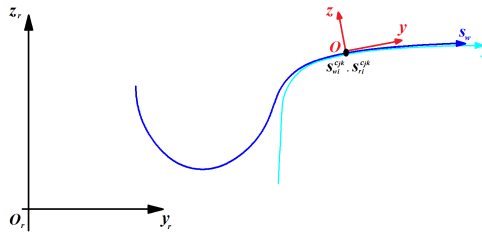

Figure 3: Normal abscissa for the wheel and rail profile.

3. *Sum on the contact points*:

$$\sum_{i=1}^{N_{PDC}} \Delta_{P_{wi}^{jk}}(s_w) = \Delta_{jk}^{w}(s_w) \tag{6}$$

where N_{PDC} represents the maximum number of contact points that can be considered for each single wheel. The output $\Delta_{jk}^{w}(s_w)$ is the removed material of the j-th wheel

during the k-th simulation of the N_c simulations derived from the statistical analysis. The number of active contact points changes during the simulation but it is usually less than N_{PDC}; thus, the amount of worn material due to non-active contact points is automatically set equal to zero.

4. *Average on the vehicle wheels and on the dynamic simulations*:

$$\sum_{k=1}^{N_c} p_k \frac{1}{N_w} \sum_{j=1}^{N_w} \Delta_{jk}^w(s_w) = \overline{\Delta}^w(s_w) \tag{7}$$

where N_w is the number of vehicle wheels while the p_k, $1 \leq k \leq N_c$, $\sum_{k=1}^{N_C} p_k = 1$ are the statistical coefficients related to the various dynamic simulations. These coefficients consider the frequency of each subtrack with respect to the whole set of the investigated mean line and they have been established by the statistical analysis. The average on the number of wheel-rail interactions has to be performed to obtain as output of the wear model a single average profile for the wheel (as required by Trenitalia and RFI).

5. *Scaling*:

Since it normally takes travelled distance of thousands kilometers in order to obtain measurable effects of wheel wear, an appropriate scaling procedure is necessary to reduce the simulated track length with a consequent limitation of the computational effort. The total mileage km_{tot} travelled by the vehicle is chosen according to the purpose of the simulations, for example equal to the re-profiling intervals. This mileage is subdivided in steps characterized by a length equal to km_{step} and the wheel profile is supposed to be constant within each discrete step (corresponding to a travelled distance equal to km_{step}). The km_{step} value represents a distance which is still too long to be simulated in reasonable computational times. However this can be overcome as follows:

- a linear relationship between the amount of worn material and the travelled distance is supposed to hold only inside the discrete step;

- according to the previous hypotheses a smaller distance km_{prove} can be simulated; then the relative amount of wheel worn material can be amplified in order to evaluate the worn material distribution relative to a km_{step} travelled distance.

The discrete step definition can be done according to two main update strategies: the constant step update strategy, which is characterized by a constant value km_{step} of the discrete step and the adaptive step update strategy, wherein the profile is updated when a given threshold Δ_{fix} on the maximum value $\Delta_{max} = \max_{s_w} \overline{\Delta}^w(s_w)$ of cumulative wear depth is reached; the value km_{step} is consequently variable.

In the present research the adaptive step approach has been chosen and the discrete step value km_{step} can be defined through the following equation:

$$km_{step} = km_{prove} \frac{\Delta_{fix}}{\Delta_{max}} \tag{8}$$

where $km_{prove} = l_{track}$ is the total travelled distance simulated during the N_c dynamic analyses. The quantity Δ_{max} represents the maximum cumulative wear depth while Δ_{fix} is the related chosen threshold value and in this work it is equal to $0.1\,\text{mm}$. The scaled

amount $\overline{\Delta}^{wsc}(s_w)$ of worn material to be removed by the wheel surface is then given by the following expression:

$$\overline{\Delta}^{wsc}(s_w) = \overline{\Delta}^w(s_w)\frac{\Delta_{fix}}{\Delta_{max}}. \tag{9}$$

6. *Smoothing of the worn material*:

$$\Im\left[\overline{\Delta}^{wsc}(s_w)\right] = \overline{\Delta}^{wsc}_{sm}(s_w); \tag{10}$$

the numerical noise and short wavelengths without physical meanings that affect the worn material distribution can be passed to the new wheel profile $\tilde{w}_n(s_w)$ with consequent problems raising in the global contact model. Hence an appropriate smoothing of the worn material distributions is required and this is achieved by means of a first-order discrete filter (i. e. a moving average filter with window size equal to $1\% \div 5\%$ of the total number of points in which the profiles are discretised); obviously the discrete filter has to conserve the mass.

7. *Profile update:*

$$\begin{pmatrix} y_w(s_w) \\ \tilde{w}_o(s_w) \end{pmatrix} - \overline{\Delta}^{wsc}_{sm}(s_w)\mathbf{n}^r_w \xrightarrow{re-parameterization} \begin{pmatrix} y_w(s_w) \\ \tilde{w}_n(s_w) \end{pmatrix}; \tag{11}$$

the last step of the procedure consists in the determination of the new wheel profile $\tilde{w}_n(s) = w_n(y)$ starting from the old one $\tilde{w}_o(s) = w_o(y)$. Due to the fact that the removal of material occurs in the normal direction to the profiles ($\mathbf{n}^r_w$ is the outgoing unit vector for the wheel profile), once the quantity $\overline{\Delta}^{wsc}_{sm}(s_w)$ has been removed, a re-parameterization of the profile must be performed to get again curve parameterized by means of the curvilinear abscissa.

5 SETTING-UP OF THE MINUETTO VIRTUAL TRACK

When the wear analyses have to be carried out on a set of tracks of considerable length by using at the same time accurate models for the vehicle and the wheel-rail contact, the utilization of a "railway line statistical model" may be an indispensable way to overcome a series of problems due to the computational times and to the setting-up of the simulations. The basic idea consists in replacing a complex railway net or the too long tracks to be simulated with a set of simpler tracks which can produce an equivalent amount and distribution of wear on the vehicle wheels. In such cases it is fundamental to sum up in a statistical model of the whole railway net the most relevant information about the real context on which the vehicles operate, in order to get results in terms of average behaviour of the vehicle-wheel profile matching considered.

The first step of the statistical approach consists in dividing the original railway line in N_c radius classes (see Tab. 2), wherein superelevation sub-classes are in turn defined; then for each radius class a representative curve has been chosen. The representative track is characterized by the mean radius R_r, the speed V_r, the superelevation h_r and the statistical weight p_k. This latter ($0 \leq p_k \leq 1$ where $1 \leq k \leq N_c$) is a weighting factor to consider the frequency of each curve with respect to the whole set of the investigated mean line. The R_r value is computed through the weighted average between the radii included in the class range $[R_m, R_M]$, using as weights the products between the lengths of the track sections and the number of weekly shifts. The

Table 2: The Minuetto virtual track.

R_m (m)	R_M (m)	R_r (m)	h_{range} (mm)	h_r (mm)	V_r (km/h)	p_k %
250	278	**263**	90–120	90	65	1.90
			130–160	160	75	4.21
278	313	**294**	90–120	90	70	1.11
			130–160	160	80	1.62
313	357	**333**	90–120	90	70	0.44
			130–160	140	80	1.24
357	417	**385**	50–80	50	70	0.80
			90–120	120	80	1.33
			130–160	150	90	4.17
417	500	**455**	50–80	80	70	1.44
			90–120	100	80	4.72
			130–160	130	90	1.29
500	625	**556**	10–40	10	70	0.14
			50–80	80	80	1.52
			90–120	90	85	2.01
			130–160	150	110	1.46
625	833	**714**	10–40	10	70	0.09
			50–80	70	85	1.56
			90–120	90	95	1.77
			130–160	130	115	0.78
833	1250	**1000**	10–40	10	70	1.10
			50–80	50	85	2.41
			90–120	120	130	2.16
			130–160	140	130	0.93
1250	2500	**1667**	0	0	70	0.17
			10–40	30	85	1.91
			50–80	80	130	1.68
			90–120	90	130	0.99
			130–160	150	130	0.17
2500	10000	**5000**	0	0	70	1.08
			10–40	20	120	1.21
			50–80	50	130	0.25
			90–120	100	130	0.004
		∞				52.3

superelevation value h_r is the one characterized by the highest sum of products between section lengths and number of weekly shifts. The representative velocity V_r is evaluated by assuming a limit value for the non-compensated acceleration a_{nc}:

$$a_{nc}^{lim} = \frac{\tilde{V}^2}{R} - g\frac{h_r}{s} \tag{12}$$

where s is the track gauge in mm and g is the gravity acceleration. Then the representative velocity V_r is chosen as the minimum value between the velocity value $\tilde{V}$ resulting from Eq. 13 and the maximum velocity V_{max} on the line:

$$V_r = \min(\tilde{V}, V_{max}). \tag{13}$$

Moreover in this work, the available data on the rail profiles provided by RFI have been exploited to select a series of rail profiles to be used as time-independent profiles in the multibody simulations. According to the working hypothesis based on the collected data that in small radius curves it is easier to find a deeply worn rail profile than in straight tracks or in large radius curves, a pair of representative worn rail profiles, in a statistical sense, has been chosen for each radius curve range.
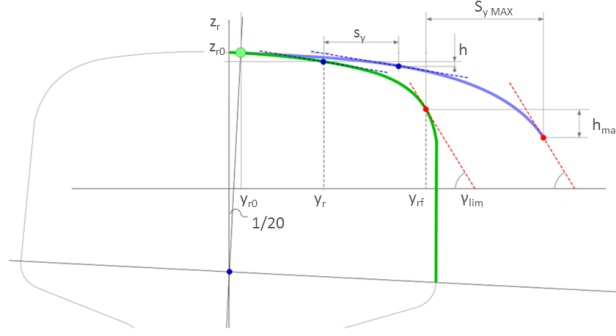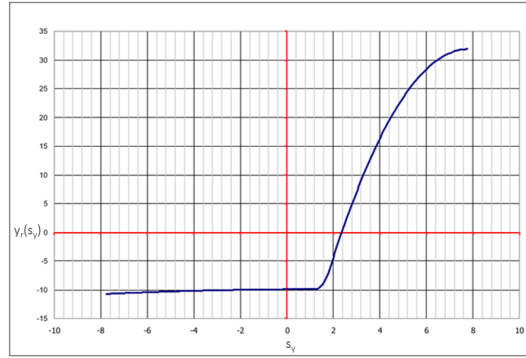
Figure 4: Design procedure of the CD1 wheel profile.

Figure 5: Graphical representation of the function $y_r(s_y)$.

6 DESCRIPTION OF THE PROPOSED WHEEL PROFILES

This section describes the procedures for the design of the two proposed wheel profiles, named CD1 and DR2 wheel profile. These procedures have been developed by the authors in collaboration with Trenitalia and RFI [19]. The CD1 wheel profile has been designed through a discrete procedure to obtain a better distribution of the contact points in the flange zone in order to improve wear characteristics and to maintain a target constant value of the equivalent conicity in a band around the nominal contact point (when the wheelset is in the neutral position). The adopted nomenclature for the wheel profile construction is shown in Fig. 4. The abscissa y_w characterizing the points of the new wheel profile is calculated starting from the abscissa y_r of the rail profile which can vary in the range $[y_{r0}, y_{rf}]$ discretized with a resolution equal to 0.1 mm and it results: $y_w = y_r(s_y) + s_y$; s_y is the variable representing the horizontal gap between wheel and rail profile and its value can vary from 0 to the maximum desired horizontal gap s_{yMAX}.

The relationship $y_r(s_y)$, occurring between the horizontal rail profile coordinate and the horizontal gap can be chosen arbitrarily; once the relationship has been defined, for each value y_r of the rail profile the corresponding value of s_y can be obtained.

In the present work, considering the purposes previously described, it has been adopted the relationship illustrated in the graphical representation of Fig. 5.

The z_w value can be evaluated from the corresponding rail value z_r: $z_w = z_r(y_r(s_y)) - h(s_y)$,

11

where the $h(s_y)$ function is defined as:

$$h(s_y) = - \int_0^{s_y} tan\left(\gamma(y_r(s'_y))\right) ds'_y. \tag{14}$$

The resulting CD1 wheel profile is illustrated in Fig. 6.
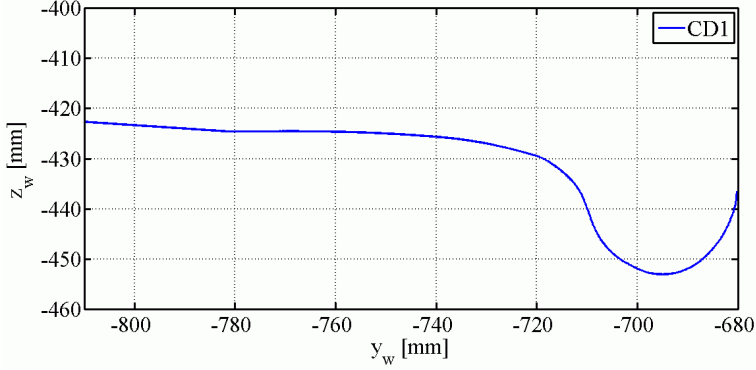

Figure 6: CD1 wheel profile.

The DR2 wheel profile is designed to guarantee the kinematic characteristics of the original matching formed by ORE S1002 wheel profile and UIC60 rail profile with laying angle α_p equal to $1/40$ rad, also with the new matching DR2 wheel profile - UIC60 rail profile canted at $1/20$ rad. The original matching has been chosen because it is widely common in European railways and it is characterised by good performances in both wear and kinematic behaviour.

The nomenclature adopted for the profile construction is shown in Fig. 7 where the apexes r and w respectively refer to auxiliary (defined on the rail plane) and local reference system (rigidly attached to the wheelset).
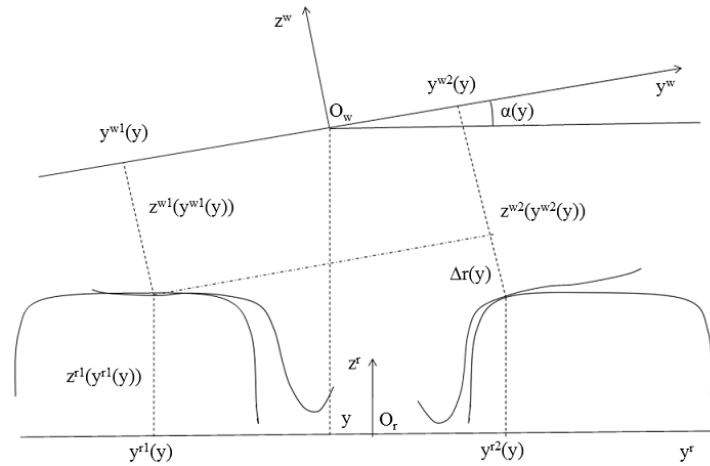
Figure 7: Adopted nomenclature for DR2 design.

The position of the local reference system origin expressed in the auxiliary reference system is denoted by $\mathbf{O}_w^r = [\ y \quad z(y)\ ]^T$.

In the present research activity, the purpose in maintaining the kinematic properties of the ORE S 1002 - UIC60 canted at $1/40$ rad matching is achieved by supposing that some variables of the new matching (DR2 wheel profile - UIC60 matching canted at $1/20$ rad) remain
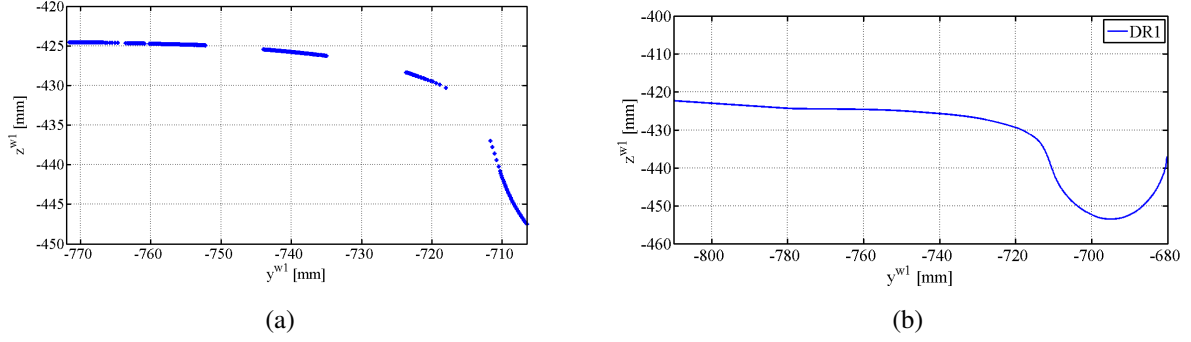
12

Figure 8: Distribution of contact points after applying the design procedure (a), the DR1 wheel profile (b).

the same of the original ones (in the remaining of the article the variables characterizing the original matching and those referring to the new matching will be respectively denoted with the subscripts 40 and 20). More specifically these variables (all depending on the wheelset lateral displacement y) are the lateral coordinates y_{r1}, y_{r2} of the contact points expressed in the auxiliary reference system, the rail functions $z_{40}^{r1}(\bullet)$, $z_{40}^{r2}(\bullet)$, the vertical coordinate z and the roll angle α of the wheelset. Consequently the design procedure requires six inputs from the old matching $y_{40}^{r1}(y)$, $y_{40}^{r2}(y)$, $\alpha_{40}(y)$, $z_{40}(y)$, $z_{40}^{r1}(\bullet)$, $z_{40}^{r2}(\bullet)$ and two inputs from the new matching $z_{20}^{r1}(\bullet)$, $z_{20}^{r2}(\bullet)$, representing the new rail functions. Then, starting from these inputs, the equations describing the coordinate transformation of the contact points between the local and the auxiliary reference system can be written both for the original matching:

$$\left(\begin{array}{c} y_{40}^{r1}(y) \\ z_{40}^{r1}(y_{40}^{r1}(y)) \end{array} \right) = \left(\begin{array}{c} y \\ z_{40}(y) \end{array} \right) + R(\alpha_{40}(y)) \left(\begin{array}{c} y_{40}^{w1}(y) \\ z_{40}^{w1}(y_{40}^{w1}(y)) \end{array} \right) \tag{15}$$

$$\left(\begin{array}{c} y_{40}^{r2}(y) \\ z_{40}^{r2}(y_{40}^{r2}(y)) \end{array} \right) = \left(\begin{array}{c} y \\ z_{40}(y) \end{array} \right) + R(\alpha_{40}(y)) \left(\begin{array}{c} y_{40}^{w2}(y) \\ z_{40}^{w2}(y_{40}^{w2}(y)) \end{array} \right) \tag{16}$$

and for the new matching:

$$\left(\begin{array}{c} y_{40}^{r1}(y) \\ z_{20}^{r1}(y_{40}^{r1}(y)) \end{array} \right) = \left(\begin{array}{c} y \\ z_{40}(y) \end{array} \right) + R(\alpha_{40}(y)) \left(\begin{array}{c} y_{20}^{w1}(y) \\ z_{20}^{w1}(y_{20}^{w1}(y)) \end{array} \right) \tag{17}$$

$$\left(\begin{array}{c} y_{40}^{r2}(y) \\ z_{20}^{r2}(y_{40}^{r2}(y)) \end{array} \right) = \left(\begin{array}{c} y \\ z_{40}(y) \end{array} \right) + R(\alpha_{40}(y)) \left(\begin{array}{c} y_{20}^{w2}(y) \\ z_{20}^{w2}(y_{20}^{w2}(y)) \end{array} \right) \tag{18}$$

where the wheelset lateral displacement value y is bounded in the range $[-y_M, y_M]$. The outputs of the design procedure that characterize the new wheel profile are the lateral $y_{20}^{w1}(y)$ (according to Eq. 17 and Eq. 18), $y_{20}^{w2}(y)$ and vertical $z_{20}^{w1}(y_{20}^{w1}(y))$, $z_{20}^{w2}(y_{20}^{w2}(y))$ coordinates of the contact points of the new wheel profile in the local reference system. The design procedure is performed in a discrete way for every y value of the discretized range $[-y_M, y_M]$ with a resolution equal to 0.1 mm.

It should be noticed that the resulting profile is characterized by holes (see Fig. 8a), that are the regions where there is not any computed contact point. In the present procedure these regions have been filled fitting the computed points with spline functions and the resulting wheel profile, named DR1, is illustrated in Fig. 8b.

The geometrical wheel/rail contact characteristics are ruled by the rolling radii difference, (the difference between rolling radii of the right and the left wheels for each lateral displacement y) defined through the following expressions respectively valid for the original (ORE S1002
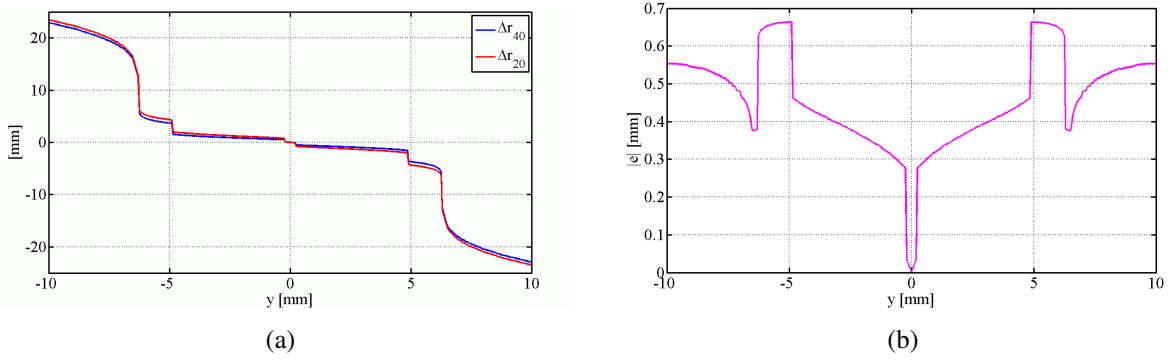
13

Figure 9: DR1-UIC60 canted at $1/20$ rad matching: rolling radii difference (a), error in rolling radii difference (b).

wheel profile and UIC60 canted at $1/40$ rad) and the resulting matching $\Delta r_{40} = z_{40}^{w2}(y_{40}^{w2}(y)) - z_{40}^{w1}(y_{40}^{w1}(y))$, $\Delta r_{20} = z_{20}^{w2}(y_{20}^{w2}(y)) - z_{20}^{w1}(y_{20}^{w1}(y))$. The adopted design procedure implies that the rolling radii difference (Fig. 9a) of the output matching is equal to the one characterizing the original matching, disregarding a small estimable variation $e = \Delta r_{20} - \Delta r_{40}$ (see Fig. 9b), calculated by means of the following analytical procedure.

Subtracting the Eq. (15) from the Eq. (16) and the Eq. (17) from the Eq. (18), it leads to the following expressions:

$$\begin{pmatrix} y_{40}^{r2}(y) - y_{40}^{r1}(y) \\ z_{40}^{r2}(y_{40}^{r2}(y)) - z_{40}^{r1}(y_{40}^{r1}(y)) \end{pmatrix} = R(\alpha_{40}) \begin{pmatrix} y_{40}^{w2}(y) - y_{40}^{w1}(y) \\ \Delta r_{40} \end{pmatrix} \tag{19}$$

$$\begin{pmatrix} y_{40}^{r2}(y) - y_{40}^{r1}(y) \\ z_{20}^{r2}(y_{40}^{r2}(y)) - z_{20}^{r1}(y_{40}^{r1}(y)) \end{pmatrix} = R(\alpha_{40}) \begin{pmatrix} y_{20}^{w2}(y) - y_{20}^{w1}(y) \\ \Delta r_{20} \end{pmatrix}. \tag{20}$$

Then, subtracting on turn the Eq. (19) from the Eq. (20) it holds:

$$R_{(\alpha_{40})}^T \begin{pmatrix} 0 \\ \Delta z_{20}^r - \Delta z_{40}^r \end{pmatrix} = \begin{pmatrix} \Delta y_{20}^r - \Delta y_{40}^r \\ \Delta r_{20} - \Delta r_{40} \end{pmatrix}. \tag{21}$$

The second component of the previous equation leads to the expression of the rolling radii functions variation between the new and the original matching:

$$(\Delta z_{20}^r - \Delta z_{40}^r) \cos \alpha_{40} = \Delta r_{20} - \Delta r_{40} = e(y) \tag{22}$$

as a function of the wheelset lateral displacement where $\Delta z_{20}^r = z_{20}^{r2}(y_{40}^{r2}(y)) - z_{20}^{r1}(y_{40}^{r1}(y))$ and Δz_{40}^r and $\Delta z_{40}^r = z_{40}^{r2}(y_{40}^{r2}(y)) - z_{40}^{r1}(y_{40}^{r1}(y))$.

In order to improve the rolling radii difference error between the original matching and DR1 wheel profile - UIC60 canted at $1/20$ rad matching, an optimization algorithm has been developed. The basic idea of this algorithm consists in translating the lateral contact points coordinates (the inputs) $y_{40}^{r1}(y)$, $y_{40}^{r2}(y)$ of a certain quantity $k(y)$, evaluated through a minimization process of the rolling radii error for each possible lateral wheelset displacement y. The lateral coordinates of the contact points in the auxiliary reference system can be then re-defined as $y_{40}^{r1^k} = y_{40}^{r1} + k$, $y_{40}^{r2^k} = y_{40}^{r2} + k$ where the k value is bounded in the range $[-\bar{k}, +\bar{k}] = I_k$. Therefore the expression of the rolling radii error becomes a function of both y and k values:

$$E(y, k) = \cos \alpha_{40}(z_{20}^{r2}(y_{40}^{r2} + k) - z_{20}^{r1}(y_{40}^{r1} + k) - z_{40}^{r2}(y_{40}^{r2}) + z_{40}^{r1}(y_{40}^{r1})). \tag{23}$$

Eq. 23 is used as the objective function to find the optimal value k_{opt} of the translation quantity, which is then defined for each wheelset lateral displacement y as:

$$k_{opt}(y) = \arg \min_{k \in I_k} |E(y, k)| . \tag{24}$$

The optimization process has been performed by discretizing the I_k range with a resolution equal to 0.1 mm. The resulting lateral coordinates of the contact points in the auxiliary reference system are evaluated as $y_{opt}^{r1} = y_{40}^{r1} + k_{opt}$, $y_{opt}^{r2} = y_{40}^{r2} + k_{opt}$. Through the introduction of these coordinates into Eq. (18) and Eq. (17), the outputs $y_{20}^{w1}(y)$, $z_{20}^{w1}(y_{20}^{w1}(y))$, $y_{20}^{w2}(y)$, $z_{20}^{w2}(y_{20}^{w2}(y))$ of the optimized wheel profile-UIC60 rail canted at $1/20$ rad matching are given by the following expressions:

$$\begin{pmatrix} y_{opt}^{r1}(y) \\ z_{20}^{r1}(y_{opt}^{r1}(y)) \end{pmatrix} = \begin{pmatrix} y \\ z_{40}(y) \end{pmatrix} + R(\alpha_{40}(y)) \begin{pmatrix} y_{20}^{w1}(y) \\ z_{20}^{w1}(y_{20}^{w1}(y)) \end{pmatrix} \tag{25}$$

$$\begin{pmatrix} y_{opt}^{r2}(y) \\ z_{20}^{r2}(y_{opt}^{r2}(y)) \end{pmatrix} = \begin{pmatrix} y \\ z_{40}(y) \end{pmatrix} + R(\alpha_{40}(y)) \begin{pmatrix} y_{20}^{w2}(y) \\ z_{20}^{w2}(y_{20}^{w2}(y)) \end{pmatrix} . \tag{26}$$

The optimized wheel profile, obtained after the holes fitting procedure and named DR2 wheel profile, is shown in Fig.10. The new rolling radii difference function is compared with the
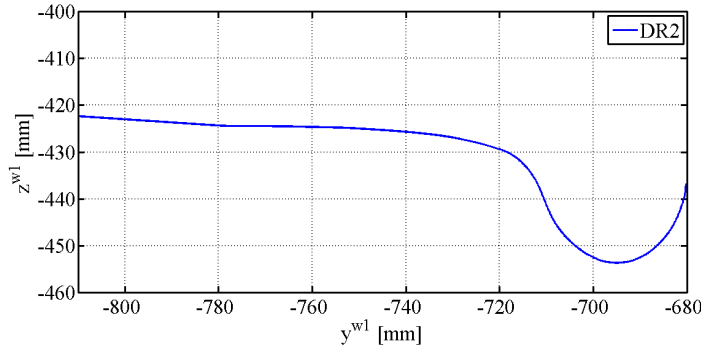

Figure 10: DR2 wheel profile.

original one in Fig. 11a; it shows that the two plots are almost coincident and that the error (see Fig. 11b), which depends on the discretization precision of the range I_k, is about zero.

The design procedure adopted to define the DR2 discrete wheel profile may be affected by numerical errors coming from different sources such as the use of splines in the holes (where there is not a contact point distribution), the fictitious points at the extremities of the wheel profile (parts of the ORE S1002 have been used) and the subsequent resamplings and smooth process of the wheel profile; moreover, since the DR2 wheel profile and UIC60 rail canted at $1/20$ rad matching is based on the geometrical properties of the ORE S 1002-UIC60 canted at $1/40$ rad, it is characterized by the stiffness caused by the conformal contact typical of the original matching. At the same time, one of the numerical advantage of the procedure consists in the fact that the new DR2 wheel profile is designed without any condition on the derivatives of the profiles; this aspect involves a reduction of the smoothing requirements and does not further increase the ill-conditioning characteristic of the design problem.
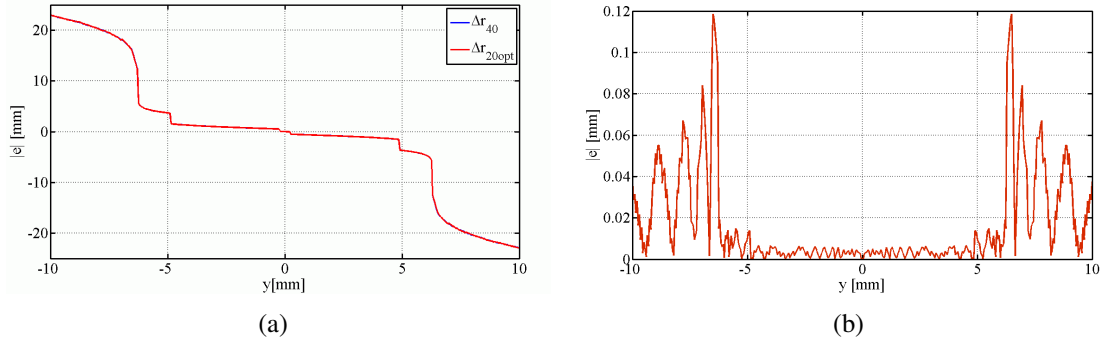
Figure 11: Characteristics of the DR2-UIC60 canted at 1/20 matching: rolling radii difference distribution (a), error in rolling radii difference distribution (b).

7 WEAR ANALYSIS

In this section the results of the dynamic simulations is presented in order to compare the evolution due to wear of the profiles considered in the present study: the standard ORE S1002 and the two innovative profiles (CD1, DR2). The wear behaviour can be evaluated through the analysis of the evolution of three reference dimensions (the qR quota, the flange thickness fT and the flange height fH, Fig. 12), according to the regulations in force [2, 1], without a complete detection of the 2D profile.
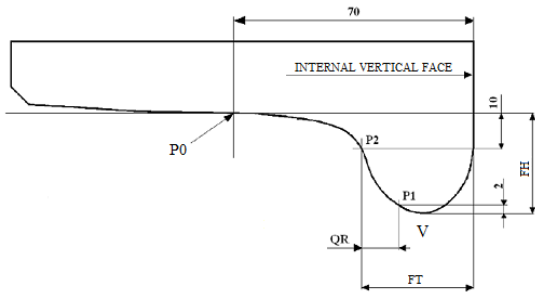
		$d \leq 630$	$630 < d \leq 760$	$760 < d$
fH	min	31.5	29.5	27.5
	max		36	

		$d \leq 760$	$760 < d \leq 840$	$840 < d$
fT	min	27.5	25	22
	max		33	

qR	min	6.5

Figure 12: Reference dimensions of the wheel profile (left) and limit values in mm (right) for a wheel having an actual rolling diameter equal to d.

The Fig. 13a shows the progress of the mean qR dimension for each profile: as it can be seen, the progress of the CD1 and DR2 profiles is slower than that of the S1002; in particular, the best performance is given by the DR2 profile. In fact, assuming a comparison limit equal to 7 mm, which is slightly above than the acceptable threshold value of 6.5 mm prescribed by the standard [2], the trend of the DR2 shows that the comparison limit is reached with an increase in the covered distance by at least 30%.

In regarding to the progress of the flange thickness fT depicted in Fig. 13b, the minimum value equal to 22 mm [2] is reached after covering about 80 000 km when the S1002 profile is adopted on the Minuetto; differently, with the new profiles the total covered distance can be extend up to 100 000 km and above. Differently from the qR, in the reduction of the flange thickness the difference between the performance provided by the CD1 and DR2 profile is about 5% only.

With respect to the evolution of the wheel shape, the comparison between the initial and the final condition for the three profiles is presented in Figg. 14a, 14b and 14c. The variation in wheel profile is numerically described by means of about one hundred procedure steps. Since
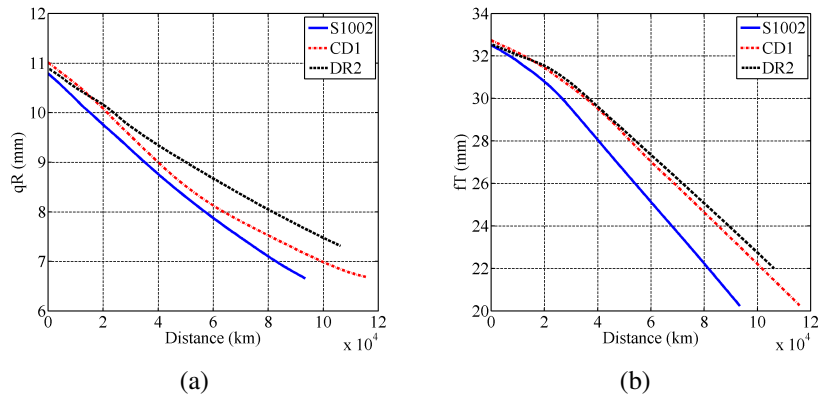
16

Figure 13: Progress of the qR dimension (a) and the flange thickness fT (b): comparison of the three wheel profiles.

the mean line of the Minuetto comprises a relevant percentage of sharp curves, the wear is mainly located on the flange instead of the tread.

It can be noticed that the two proposed wheel profiles, CD1 and DR2, exhibit a more uniform wear distribution along the wheel profile, while in the ORE S1002 profile wear mainly arises on the wheel flange zone.

8 CONCLUSIONS

In this paper the authors have presented a work focused on the development of a mathematical model for the wear evaluation in railway vehicles and on the comparison between the performance provided by different wheel profiles in wear behaviour and running stability. More specifically, the standard ORE S1002 wheel profile (matched to the UIC60 rail profile canted at $1/20$ rad)) widely used on vehicles in service on the Italian railway line has been compared with two innovative wheel profiles developed by the authors in order to improve the poor performance of the S1002 profile in wear and behaviour and guidance in sharp curves. This whole research has been performed in collaboration with Trenitalia S.p.A and Rete Ferroviaria Italiana which provided the necessary technical and experimental data.

The two innovative wheel profiles designed in the present activity to the UIC60 rail with a cant of $1/20$ rad have proven to work fine as for the resistance to wear if compared with the S1002 wheel profile.

Future developments of the present study will consist in the experimental evaluation of the wear evolution on Minuetto vehicle equipped with the new wheel profiles, to verify the progress of the reference dimensions. To this end, experimental tests have been scheduled by Trenitalia and will be soon carried out; after choosing a particular track, a few vehicles having the same weekly shift will be equipped with the three profiles described in this work in order to compare their performance both in terms of wear behaviour and running stability.
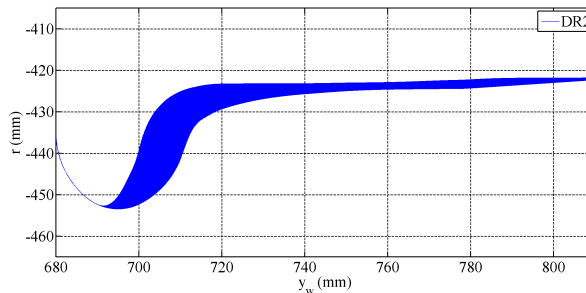
17
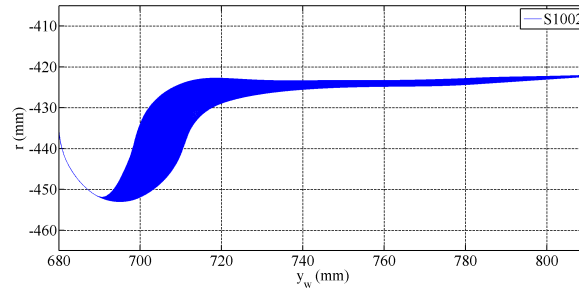
(a) S1002.
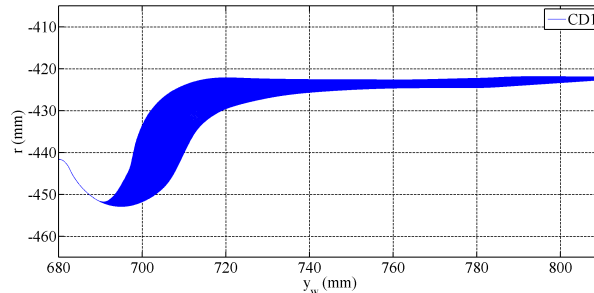
(b) CD1.

(c) DR2.

Figure 14: Wear progress on the three wheel profiles.

REFERENCES

[1] EN 14363: Railway applications — Testing for the acceptance of running characteristics of railway vehicles — Testing of running behaviour and stationary tests, 2005.

[2] EN 15313: Railway applications — In-service wheelset operation requirements — In-service and off-vehicle wheelset maintenance, 2010.

[3] J-F. Antoine, C. Visa, C. Sauvey, and G. Abba. Approximate analytical model for hertzian elliptical contact problems. *Journal of Tribology*, 128:660–664, 2006.

[4] J. Auciello, E. Meli, S. Falomi, and M. Malvezzi. Dynamic simulation of railway vehicles: wheel/rail contact analysis. *Vehicle System Dynamics*, 47:867–899, 2009.

[5] M. Bozzone, E. Pennestrì, and P. Salvini. A lookup table-based method for wheel-rail contact analysis. *Proceedings of the Institution of Mechanical Engineers, Part K: Journal of Multibody Dynamics*, 225:127–138, 2010.

[6] F. Braghin, R. Lewis, R. S. Dwyer-Joyce, and S. Bruni. A mathematical model to predict railway wheel profile evolution due to wear. *Wear*, 261:1253–1264, 2006.

[7] R. Enblom and M. Berg. Simulation of railway wheel profile development due to wear influence of disc braking and contact environment. *Wear*, 258:1055–1063, 2005.

[8] C. Esveld. *Modern Railway Track*. Delft University of Technology, Delft, Netherland, 2001, 1985.

[9] H. Hertz. The contact of elastic solids. *J. Reine Angew. Math.*, 92:156–171, 1881.

[10] M. Ignesti, M. Malvezzi, L. Marini, E. Meli, and A. Rindi. Development of a wear model for the prediction of wheel and rail profile evolution in railway systems. *Wear*, 2012. DOI: 10.1016/j.wear.2012.01.020.

[11] S. Iwnicki. Simulation of wheel - rail contact forces. *Fatigue and Fracture of Engineering Materials and Structures*, 26:887–900, 2003.

[12] J. J. Kalker. Survey of wheel-rail rolling contact theory. *Vehicle System Dynamics*, 8:317–358, 1979.

[13] J. J. Kalker. A fast algorithm for the simplified theory of rolling contact. *Vehicle System Dynamics*, 11:1–13, 1982.

[14] J. J. Kalker. *Three-dimensional Elastic Bodies in Rolling Contact*. Kluwer Academic Publishers, Dordrecht, Netherlands, 1990.

[15] E. Meli, S. Falomi, M. Malvezzi, and A. Rindi. Determination of wheel - rail contact points with semianalytic methods. *Multibody System Dynamics*, 20:327–358, 2008.

[16] O. Polach. Influence of wheel/rail contact geometry on the behaviour of a railway vehicle at stability limit. pages 2203–2210, The Netherlands, August 2005. ENOC-2005, Eindhoven University of Technology, 7-12 August.

[17] J. Pombo, J. Ambrosio, M. Pereira, R. Lewis, R. Dwyer-Joyce, C. Ariaudo, and N. Kuka. A study on wear evaluation of railway wheels based on multibody dynamics and wear computation. *Multibody System Dynamics*, 24:347–366, 2010.

[18] A. A. Shabana, M. Tobaa, H. Sugiyama, and K. E. Zaazaa. On the computer formulations of the wheel/rail contact problem. *Nonlinear Dynamics*, 40:169–193, 2005.

[19] P. Toni. Ottimizzazione dei profili delle ruote su binario con posa 1/20. Technical report, Trenitalia S.p.A., 2010.